Наносистеми, наноматеріали, нанотехнології
Nanosistemi, Nanomateriali, Nanotehnologii
2025, т. 23, № 1, сс. 191–202
https://doi.org/10.15407/nnn.23.01.0191

PACS numbers: 78.67.Bf, 81.07.Nb, 81.16.Fg, 87.19.xb, 87.64.Ee, 87.64.K-, 87.85.Rs

Preparation of Metal-Complexes' Nanoparticles Derivative from Novel Schiff Bases of Furan and Pyridine

Mohammad Taher Al-Omar and Mohammad Moudar Al-khuder

Department of Chemistry,
Homs University
(formerly AL-Baath University),
Homs, Syria

Heterocyclic compounds have great importance in the medical and industrial fields. Furan and pyridine are most widespread and effective of these compounds. In this study, we prepare two novel Schiff bases 1,1′(1,4-phenylene)bis(N-(4-((pyridin-2-ylmethylene)amino)phenyl)methaneimine (L_1), 1,1′-(1,4-phenylene)bis(N-(4-((furan-2-ylmethylene)amino)phenyl)methanimine) (L_2), and their metal complexes with (Cd^{2+}, Mn^{2+}, Sn^{2+}). The prepared compounds are characterized using ^{1}H-NMR, ^{13}C-NMR, UV–Vis, FT-IR, and SEM techniques. As a result, all the metal complexes are bimetallic and non-electrolytic. In addition, the biological activity against *Escherichia coli* and *Staphylococcus aureus* bacteria is studied for the prepared compounds.

Гетероциклічні сполуки мають велике значення в медицині та промисловості. Фуран і піридин є найбільш поширеними й ефективними з цих сполук. В цьому дослідженні ми підготували дві нові Шиффові основи 1,1′(1,4-фенілен)біс(N-(4-((піридин-2-ілметилен)аміно)феніл)метанеімін (L_1), 1,1′-(1,4-фенілен)біс(N-4-((фуран-2-ілметилен)аміно)феніл)метанімін (L_2), а також їхні металічні комплекси з (Cd^{2+}, Mn^{2+}, Sn^{2+}). В результаті всі металокомплекси були біметалічними та неелектролітними. Також було вивчено біологічну активність одержаних сполук щодо бактерій *Escherichia coli* та *Staphylococcus aureus*.

Key words: pyridine aldehyde, furfural, 1,4-diaminobenzene, terephthal aldehyde, metal complexes.

Ключові слова: піридиновий альдегід, фурфурол, 1,4-діамінобензол, терефталевий альдегід, комплекси металів.

(Received 4 December, 2023; in revised form, 14 December, 2023)

1. INTRODUCTION

The processes of designing drugs from organic compounds with new and practically important biological behaviours is required organic interactions involving the condensation of two or more types of molecules to obtain a new derived from imine compounds as a commonly used compounds for this purpose [1–3]. The reaction of condensation of the primary amines with aldehydes or ketones gives an important product. The Schiff base reaction was done under normal conditions. The presence of a Schiff base in our interactions is of great importance due to the stability of complexes of metal ions with different oxidation states and because of its involvement in many vital processes on a large scale such as industrial fields and as catalysts for reactions in addition to its significant wide involvement in biological activities [4]. The stable structure of metal complexes is attributed to the nitrogen lone pair electrons on azomethine (–N=CH) bonding [5]. Donor atoms of Schiff base ligand can be enhanced the antibacterial activity through the coordination to metal ions [6, 7]. The interaction of metal ions with Schiff base ligands can give structures of different geometric shapes and have various applications such as their use in organometallic chemistry as catalysts, and for the design of important medicinal compounds as anti-tumour, anticancer, anti-bacterial, anti-fungal agents, antiviral agents [8, 9]. The presence of heterocyclic (pyridine and furan) increases the effectiveness of the Schiff bases ligands. Many studies have dealt with the preparation of different compounds based on furan and pyridine [10–16].

In this paper, we aim to prepare (Cd(II), Sn(II), and Mn(II)) complexes with the two new ligands derived from furan and pyridine.

2. EXPERIMENTAL

2.1. Materials and Apparatus

All chemicals used in this work were purchased from BDH, Aldrich and Merck companies and were used without further purification.

NMR spectra were recorded on a Brucker instrument (400 MHz) spectrometer. Chemical shifts were reported in (δ) ppm relative to tetramethylsilane (TMS). Data were reported as follow: chemical shift, multiplicity, coupling constant (Hz), integration, and assignment. FT-IR spectra (ν, cm^{-1}) were recorded on a JASCO Spectrum FT-IR 4100 spectrometer using KBr pellets. UV-Vis spectroscopy were measured by using Jasco-V630-UV-Vis at the wavelength range 200–800 nm, using match quartz cells (1 cm) and DMSO as a solvent.

2.2. Synthesis of Ligand 1,1 (1,4-Phenylene)bis(N-(4-((Pyridin-2-Ylmethylene)Amino)Phenyl)Methaneimine (L_1)

The ligand (L_1) was prepared from the compound (PMAD) according to Fig. 1.

In a clean tow-necked round bottom flask 100 mL equipped with a magnetic stir and reflux condenser, PMAD (0.661 g (2.1 mmol)) and 50 mL of ethanol were gradually added into the flask and stirred at 55°C until completely dissolving. picolinaldehyde (0.422 mL (4.2 mmol)) dissolved in 10 mL of ethanol was added into the flask, after 10 min of stirring at same previous temperature, then the mixture heated up to 78°C and stirred for 6 h, while the reaction was monitored through TLC technique. After that, the resulting mixture was stirred for 24 h at room temperature. Finally, the solution was cooled, and then the precipitate was filtered and left to dry giving a yellow precipitate, and recrystallized using hot ethanol. The yield of the product was found to be 72.65%.

2.3. Synthesis of (L_1) Metal Complexes

L_1 (0.123 g (0.25 mmol)) was dissolved in 25 mL of ethanol in a clean tow-necked round bottom flask 250 mL equipped with a magnetic stir and reflux condenser. (0.5 mmol) of metal chloride MCl_2 ($M = Mn^{2+}$, Sn^{2+}, Cd^{2+}) was dissolved in 10 mL of ethanol and added

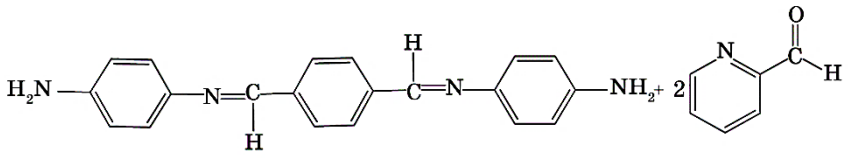

4.4′((1.4-phenylenebis(methaneylylidene))bis(azaneylylidene))dianiline (PMAD)

Picolinaldehyde

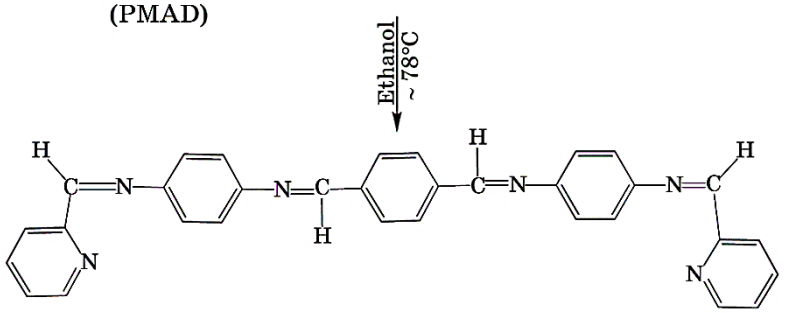

1.1′-(1.4-phenyllene)bis(*N*-(4-((pyridin-2-ylmethylene)amino)phenyl)methanimine) (L_1)

Fig. 1. General reaction scheme for synthesizing of L_1.

drop by drop to the ligand solution, pH was adjusted at 7 using triethylamine, after that the mixture stirred at 78°C for 3 h. The produced precipitate was filtered, washed with ethanol, then, diethyl ether, dried, and weighted. Figure 1 describes the chemical reaction.

2.4. Synthesis of Ligand 1,1 -(1,4-Phenylene)bis(N-(4-((Furan-2-Ylmethylene)Amino)Phenyl)Methanimine) (L_2)

The ligand (L_2) was prepared from the compound (PMAD) according to Fig. 2. In a clean tow-necked round bottom flask 100 mL equipped with a magnetic stir and reflux condenser, PMAD (1.33 g (4.2 mmol)) and 50 mL of ethanol were gradually added into the flask and stirred at 60°C until completely dissolving. Furfural (0.850 mL (8.4 mmol)) dissolved in 15 mL of ethanol was added into the flask; after 10 min of stirring at same previous temperature, then, the mixture heated up to 78°C and stirred for 5 h, while the reaction was monitored through TLC technique. After that, the resulting mixture was stirred for 24 h at room temperature. Finally, the solution was cooled, and the precipitate was filtered and left to dry giving a brownish yellow precipitate, and recrystallized using hot ethanol. The yield of the product was found to be 92.96%.

2.5. Synthesis of (L_2) Metal Complexes

L_1 (0.117 g (0.25 mmol)) was dissolved in 25 mL of ethanol in a clean tow-necked round bottom flask 250 mL equipped with a magnetic stir and reflux condenser. 0.5 mmol of metal chloride MCl_2 (M = Mn, Sn, Cd) was dissolved in 10 mL of ethanol and added drop-by-drop to the ligand solution; pH was adjusted at 7 using tri-

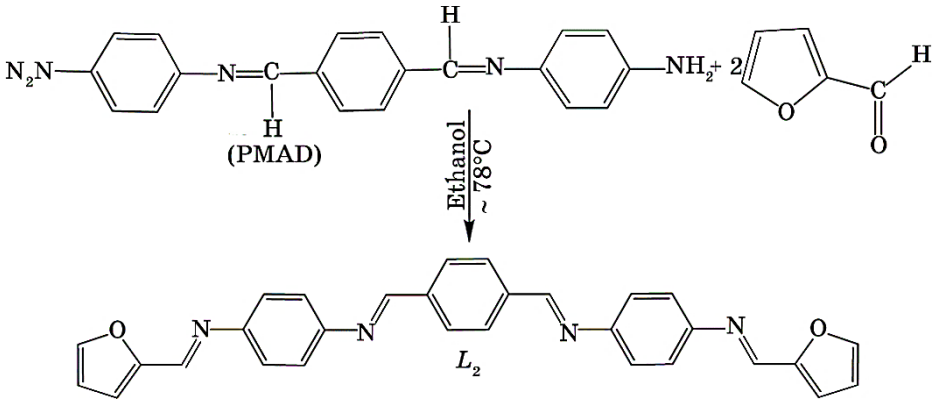

Fig. 2. General reaction scheme for synthesizing of L_2.

TABLE 1. The yield and physical properties of the produced compounds.

Compound	Formula	M, g·mol^{-1}	Colour	Yield, %	M, % found (calc)
L_1	$C_{32}H_{24}N_6$	492.59	Yellow	72.65	—
$Mn_2L_1Cl_4$	$Mn_2C_{32}H_{24}N_6Cl_4$	744.27	Light brown	67.07	13.50 (14.76)
$Cd_2L_1Cl_4$	$Cd_2C_{32}H_{24}N_6Cl_4$	859.23	Light yellow	70.23	24.33 (26.16)
$Sn_2L_1Cl_4$	$Sn_2C_{32}H_{24}N_6Cl_4$	871.81	Light yellow	48.85	26.17 (27.23)
L_2	$C_{30}H_{22}N_4O_2$	470.53	Brownish yellow	92.96	—
$Mn_2L_2Cl_4$	$Mn_2C_{30}H_{22}N_4O_2Cl_4$	722.21	Light brown	73.18	14.30 (15.21)
$Cd_2L_2Cl_4$	$Cd_2C_{30}H_{22}N_4O_2Cl_4$	837.17	Brownish yellow	75.96	24.50 (26.85)
$Sn_2L_2Cl_4$	$Sn_2C_{30}H_{22}N_4O_2Cl_4$	849.75	Brownish yellow	58.05	26.87 (27.93)

ethylamine; after that, the mixture stirred at 78°C for 3 h. The produced precipitated was filtered, washed with ethanol then diethyl ether, dried and weighted.

Melting point was determined using thermometer, which was of > 300°C for all compounds. Electrical conductivity has been also measured for all metal complexes, and it was below 80 μs, so, we concluded that all the prepared metal complexes ware non-electrolyte.

Silver nitrate solution as an indicator was used to determination of chloride ions, the results shows the chloride ions linked with metal ions in the co-ordination sphere, while the metallic calculations showed that all complexes were bimetallic. The physical properties of the prepared compounds were arranged in the Table 1.

3. RESULTS AND DISCUSSION

3.1. NMR Characterization

L_1 and L_2 compounds were characterized using H-NMR, C-NMR.

(L_1): ^{1}H-NMR (400 MHz, DMSO): δ 6.628–7.668 (*m*, 6H), 7.861–8.167 (*m*, 3H), 8.595–8.860 (*m*, 3H) ppm; ^{13}C-NMR (125 MHz, DMSO): δ 114.565, 120.790, 122.797, 123.495, 124.985, 126.731, 137.161, 138.781, 149.322, 149.889, 154.237, 155.529, 160.880 ppm.

(L_2): ^{1}H-NMR (400 MHz, DMSO): δ 6.712–6.725 (*m*, 1H), 6.783–

6.796 (*m*, 1H), 7.150–7.161 (*m*, 2H), 7.321 (*s*, 2H), 7.542–7.7553 (*m*, 1H), 7.950–7.955 (*m*, 2H), 8.492 (*s*, 1H), 9 (*s*, 1H) ppm; ^{13}C-NMR (125 MHz, DMSO): δ 113.029, 113.388, 117.374, 122.474, 130.683, 142.827, 146.878, 148.158, 149.515, 149.665, 152.531, 161.052 ppm.

3.2. FT-IR Characterization

3.2.1. FT-IR of L_1 Ligand and Its Complexes

The FT-IR spectrum of L_1 compared with PMAD are presented in Fig. 3, where the IR spectrums showed that the disappearance of the absorption band at 3374, 3338 cm^{-1} belongs to N–H_2 bond of the PMAD; also a new band appears at 1585 cm^{-1} belongs to (C=N) in the pyridine ring confirming that the condensation reaction between the PMAD and picolinaldehyde has occurred. On the other hand, the metal complexes IR spectra shows shifting of absorption band of azomethine (C=N) and pyridine (C=N). The most important IR data of L_1 ligand and its complexes are summarized in Table 2.

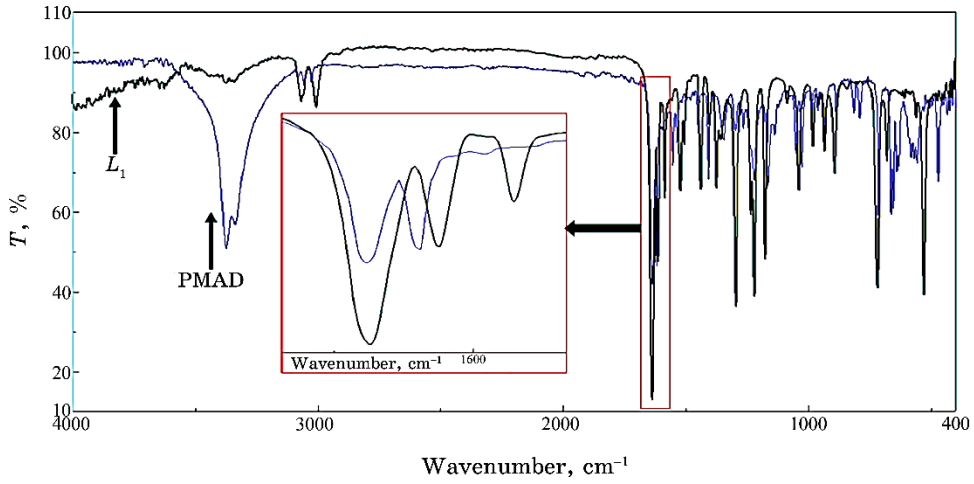

Fig. 3. FT-IR spectrum of L_1 compared with PMAD.

TABLE 2. The absorption bands of L_1 and its complexes.

Compound	ν(C=N)	ν(C=N)	ν(C=N) pyridine
L_1	1637	1612	1585
$Mn_2L_1Cl_4$	1636	1590	1552
$Cd_2L_1Cl_4$	1631	1586	1561
$Sn_2L_1Cl_4$	1639	1587	1553

3.2.2. FT-IR of L_2 Ligand and Its Complexes

The FT-IR spectrum of L_2 compared with PMAD presented in Fig. 4, where the IR spectrums showed that the disappearance of the absorption band at 3374, 3338 cm^{-1} belongs to N–H_2 bond of the PMAD; also a new band appears at 1245 cm^{-1} belongs to (C–O) in the furan ring confirming that the condensation reaction between the PMAD and furfural has occurred. On the other hand, the metal complexes IR spectra shows shifting of absorption band of azomethine (C=N) and (C–O). The most important IR data of L_2 ligand and its complexes are summarized in Table 3.

3.3. UV–Vis Characterization

The electronic spectra of L_1 and L_2 ligands and their complexes showing the electronic transformation between energy levels are presented in Figs. 5 and 6 with the UV–Vis of L_1 ligand and its complexes and of L_2 ligand and its complexes, respectively.

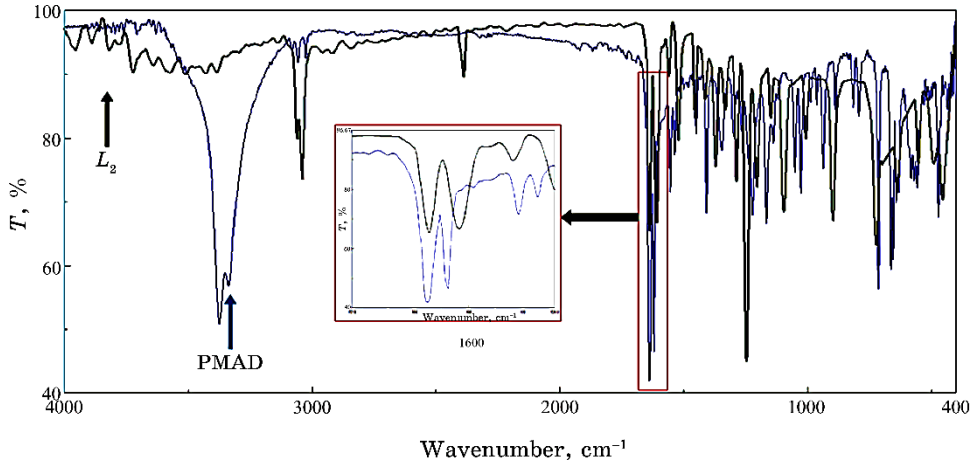

Fig. 4. FT-IR spectrum of L_2 compared with PMAD.

TABLE 3. The absorption bands of L_2 and its complexes.

Compound	ν(C=N)	ν(C=N)	ν(C–O)
L_2	1636	1609	1245
$Mn_2L_2Cl_4$	1638	1576	1214
$Cd_2L_2Cl_4$	1640	1580	1216
$Sn_2L_2Cl_4$	1634	1588	1219

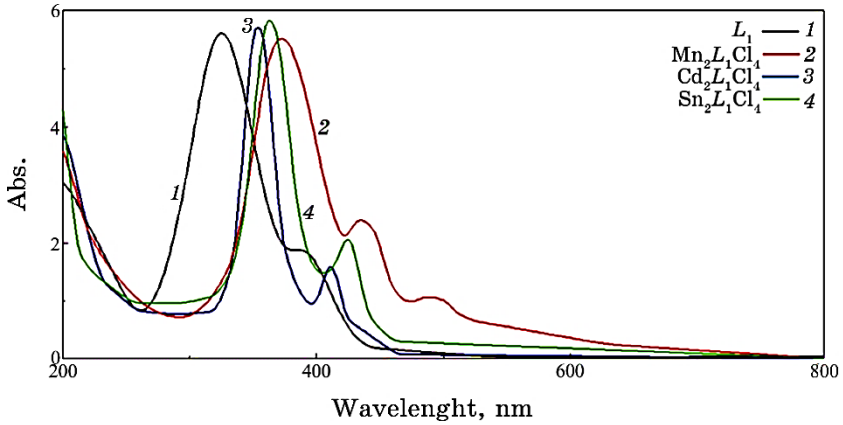

Fig. 5. UV–Vis spectrum of L_1 and its complexes.

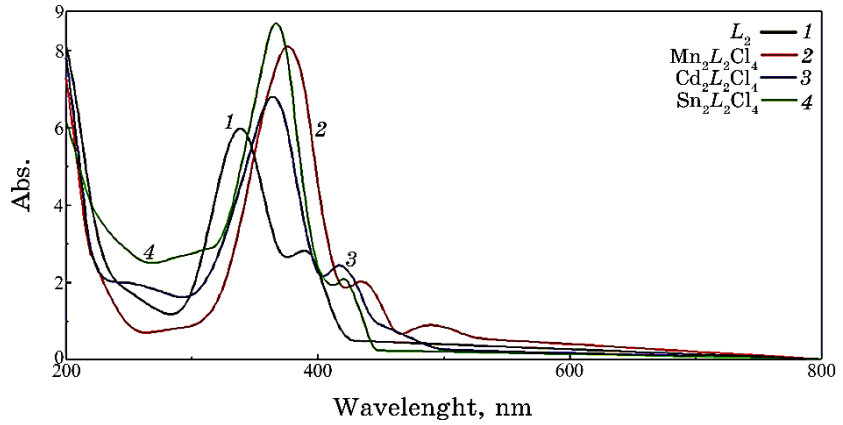

Fig. 6. UV–Vis spectrum of L_2 and its complexes.

TABLE 4. The electronic transitions for L_1, L_2 and their complexes.

Compound	$\pi \rightarrow \pi^*$	$n \rightarrow \pi^*$	$d \rightarrow d$
L_1	326	384	—
$Mn_2L_1Cl_4$	372	434	488
$Cd_2L_1Cl_4$	354	410	—
$Sn_2L_1Cl_4$	362	424	—
L_2	338	390	—
$Mn_2L_2Cl_4$	376	434	490
$Cd_2L_2Cl_4$	364	418	—
$Sn_2L_2Cl_4$	366	420	—

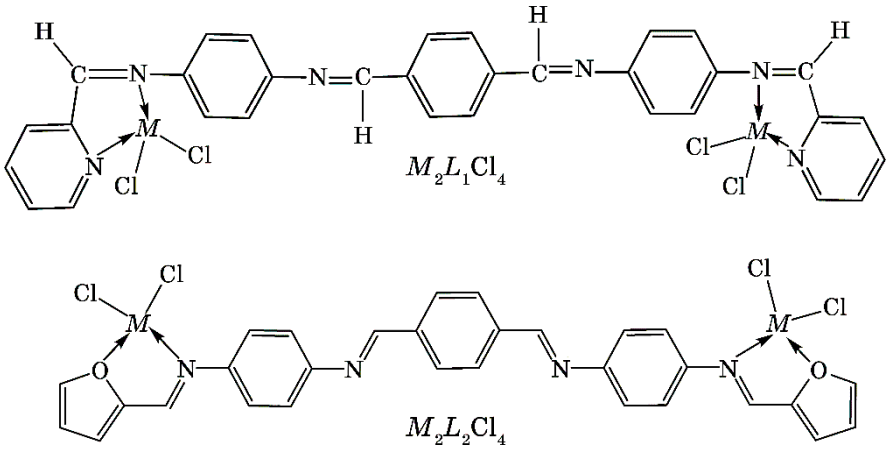

Fig. 7. Structures for the L_1 and L_2 complexes ($M = Mn^{2+}$, Cd^{2+}, Sn^{2+}).

The obtained data from UV–VIS spectra are arranged in the Table 4. Therefore, we can assume the structures for the L_1 and L_2 complexes as showed in Fig. 7.

3.4. SEM Characterization

Scanning electron microscopy technique was used to analyse the surface morphology of metal complexes (Fig. 8 represents SEM image of $Cd_2L_1Cl_4$ complex; the particles' sizes are in nanoscale range).

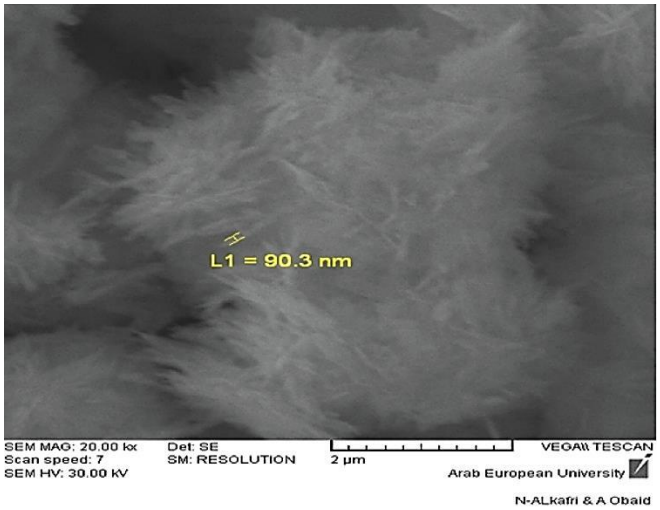

Fig. 8. SEM image of $Cd_2L_1Cl_4$ complex.

3.5. Antibacterial Activity Study

The antibacterial efficacy of the prepared compounds was tested against *Escherichia coli*, and *Staphylococcus aureus* bacteria comparing with gentamicin (as a reference). Two different concentrations (50 and 1000 mg/ml) of the compounds and gentamicin have been selected for antibacterial assay. In our research, we chose to study *E. coli* and *S. aureus* bacteria, because of their wide spread in society so they affect in the daily life of humans, as *Escherichia* is a common bacterium found in the intestines of humans and warm-blooded animals. It is often used as an indicator for faecal contamination in water and soil [17].

Pathogenic strains of *E. coli* are often transmitted through contaminated food or water [18] and can be particularly dangerous for young children, elderly individuals, and those with weakened immune systems. This bacterium can cause a range of infections, including intestinal, skin, wound sepsis, septicaemia, neonatal septicaemia, and urinary tract infections [19]. Studies have shown that some non-steroidal pain relievers, such as diclofenac sodium, can play an inhibitory role in the growth of some bacteria, whether negative or positive, in addition to using it as an anti-inflammatory [20, 21].

E. coli is also commonly used in scientific research, as it is easy to grow and manipulate in the laboratory. It has been used as a model organism for studying various biological processes, and has contributed to many important discoveries in microbiology and genetics [22], while *S. aureus* is a major bacterial human pathogen that causes a wide variety of clinical manifestations. Infections are common both in community-acquired as well as hospital-acquired settings and treatment remains challenging to manage due to the emergence of multidrug resistant strains such as MRSA (methicillin-resistant *S. aureus*) [23]. *S. aureus* is found in the environment and is also found in normal human flora, located on the skin and mucous membranes (most often the nasal area) of most healthy individuals. *S. aureus* does not normally cause infection on healthy skin; however, if it is allowed to enter the bloodstream or internal tissues, these bacteria may cause a variety of potentially serious infections [24]. Transmission is typically from direct contact. However, some infections involve other transmission methods [25].

The results are arranged in Table 5 and presented graphically in the bar graph (Fig. 9).

4. CONCLUSION

In summary, two new Schiff bases ligands and their metal complexes were successfully prepared and characterized using ^{1}H-NMR, ^{13}C-NMR, UV–Vis, FT-IR and SEM methods, which indicate the bimetallic structure in the metal complexes formula, the particle size of the com-

TABLE 5. Biological test results of the *E. coli* and *S. aureus*.

Entry	50, μg/mL		100, μg/mL	
	E. coli	*S. aureus*	*E. coli*	*S. aureus*
L_1	8	9	10	11
$Cd_2L_1Cl_4$	12	14	14	16
$Mn_2L_1Cl_4$	15	17	16	16
$Sn_2L_1Cl_4$	13	15	14	15
L_2	11	13	13	15
$Cd_2L_2Cl_4$	13	14	16	18
$Mn_2L_2Cl_4$	16	17	17	17
$Sn_2L_2Cl_4$	14	16	15	16
gentamicin	22	25	25	26
DMSO	0	0	0	0

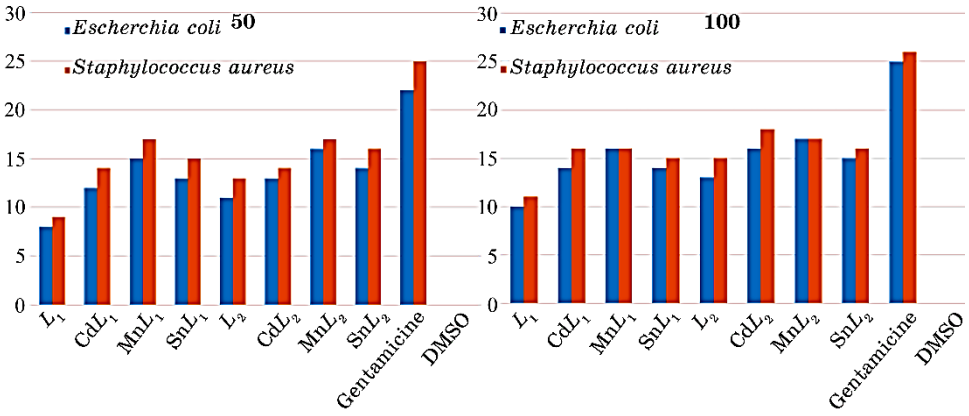

Fig. 9. Biological activity of prepared compounds.

plexes were in nanoscale. In addition, the biological activity against *Escherichia coli* and *Staphylococcus aureus* bacteria was studied; it was found that the prepared metal complexes have more biologically activity than Schiff bases ligands, which promises with amazing results for the prepared compounds in various pharmacological applications.

REFERENCES

1. S. Manivel, S. B. Gangadharappa, N. Elangovan, R. Thomas, O. A. Abu Ali, and D. I. Saleh, *J. Mol. Liq.*, **350**: 118531(2022); https://doi.org/10.1016/j.molliq.2022.118531
2. A. Z. El-Sonbati, W. H. Mahmoud, G. G. Mohamed, M. A. Diab, S. M. Morgan,

and S. Y. Abbas, *Appl. Organomet. Chem.*, **33**, Iss. 9: e5048 (2019); https://doi.org/10.1002/aoc.5048
3. Y. Badeea, W. Mahdi, Y. Ibrahim, and F. Musa, *Int. J. Drug. Deliv. Technol.*, **11**, Iss. 3: 1 (2021).
4. S. De, A. Jain, and P. Barman, *Chemistry Select*, **7**, Iss. 7: e202104334 (2022); https://doi.org/10.1002/slct.202104334
5. M. Sameer Al-Rawi, and F. Abed Nashaan, *Chem. Methodol.*, **7**: 106 (2023). https://doi.org/10.22034/CHEMM.2023.362512.1610
6. H. M. A. Al-Redha, S. H. Ali, and S. S. Mohammed, *Baghdad Sci. J.*, **19**, Iss. 3: 704 (2022); http://dx.doi.org/10.21123/bsj.2022.19.3.0704
7. S. K. Sahib and L. K. Abdul Karem, *Baghdad Sci. J.*, **17**, Iss. 1: 99 (2020); http://dx.doi.org/10.21123/bsj.2020.17.1.0099
8. S. Mathan Kumar, J. Rajesh, K. Anitha, K. Dhahagani, M. Marappan, N. Indra Gandhi, and G. Rajagopal, *Spectrochimica Acta. Part A: Mol. Biomol. Spectrosc.*, **142**: 292 (2015); https://doi.org/10.1016/j.saa.2015.01.080
9. P. Elena, F. Julea, Y. Chumakov, P. Petrenco, T. Roşu, and A. Gulea, *J. Organomet. Chem.*, **836–837**: 44 (2017); https://doi.org/10.1016/j.jorganchem.2017.01.018
10. C. R. Sahoo, S. K. Paidesetty, B. Dehury, and R. N. Padhy, *J. Biomol. Struct. Dyn.*, **55**: 1 (2023); https://doi.org/10.1080/07391102.2023.2217918
11. A. Kumar and A. Kumar, *Sci. Temper.*, **14**, Iss. 1: 20 (2023); https://doi.org/10.58414/SCIENTIFICTEMPER.2023.14.1.04
12. X. Tang, Z. Zhang, L. Jing, K. Luan, S. Zhou, and T. Zhang, *Cellulose*, **30**: 10519 (2023); https://doi.org/10.1007/s10570-023-05510-3
13. D. T. Nguyen, T. N. Nguyen, and T. V. Pham, *Vietnam J. Catal. Adsorpt.*, **12**, Iss. 1: 49 (2023); https://doi.org/10.51316/jca.2023.008
14. Ö. Altun and M. Ö. Koçer, *J. Mol. Struct.*, **1224**: 129242 (2021); https://doi.org/10.1016/j.molstruc.2020.129242
15. N. S. Hassan and W. K. Mahdi, *Chem. Methodol.*, **7**: 419 (2023); https://doi.org/10.22034/CHEMM.2023.385342.165
16. M. Ilakiyalakshmi, S. R. Mohana, and N. A. Arumugam, *Inorg. Chem. Commun.*, **157**: 111412 (2023); https://doi.org/10.1016/j.inoche.2023.111412
17. S. Ishii and M. J. Sadowsky, *Microbes Environ.*, **23**, Iss. 2: 101 (2008); https://doi.org/10.1264/jsme2.23.101
18. Ø. Olsvik, Y. Wasteson, A. Lund, and E. Hornes, *Int. J. Food Microbiol.*, **12**, Iss. 1: 103 (1991); https://doi.org/10.1016/0168-1605(91)90051-P
19. M. Rostami-Yazdi, B. Clement, and U. Mrowietz, *Arch. Dermatol. Res.*, **302**: 531 (2010); https://doi.org/10.1007/s00403-010-1061-4
20. S. G. Dastidar, K. Ganguly, K. Chaudhuri, and A. Chakrabarty, *Int. J. Antimicrob. Agents*, **14**, Iss. 3: 249 (2000); https://doi.org/10.1016/S0924-8579(99)00159-4
21. A. Laudy, E. Kulińska, and S. Tyski, *Molecules*, **22**, Iss. 1: 114 (2017); https://doi.org/10.3390/molecules22010114
22. G. L. Rosano, E. S. Morales, and E. A. Ceccarelli, *Protein Sci.*, **28**, Iss. 8: 1412 (2019); https://doi.org/10.1002/pro.3668
23. H. W. Boucher and G. R. Corey, *Clin. Infect. Dis.*, **46**, Iss. 5: S344 (2008); https://doi.org/10.1086/533590
24. F. D. Lowy, *N. Engl. J. Med.*, **339**: 520 (1998); https://doi.org/10.1056/NEJM199808203390806
25. J.-P. Rasigade and F. Vandenesch, *Infect. Genet. Evol.*, **21**: 510 (2014); https://doi.org/10.1016/j.meegid.2013.08.018